Pharmaceutical Research, Vol. 23, No. 10, October 2006 (© 2006)
DOI: 10.1007/s11095-006-9047-9

Research Paper

A Comparison of the Physical Stability of Amorphous Felodipine and Nifedipine Systems

Patrick J. Marsac,[1] Hajime Konno,[1,2] and Lynne S. Taylor[1,3]

Received January 16, 2006; accepted May 1, 2006; published online August 23, 2006

Purpose. The objective of this study was to investigate thermodynamic and kinetic factors contributing to differences in the isothermal nucleation rates of two structurally related calcium channel blockers, nifedipine and felodipine, both alone and in the presence of poly(vinylpyrrolidone) (PVP).
Materials and Methods. Thin films of amorphous systems were cast onto glass slides and the nucleation rate was determined using optical microscopy. Enthalpy, entropy, and free energy of crystallization of the pure compounds were measured using differential scanning calorimetery (DSC). Molecular mobility and glass transition temperature of each amorphous system were characterized using DSC and hydrogen bonding patterns were analyzed with infrared spectroscopy. The composition dependence of the thermodynamic activity of the amorphous drug in the presence of the polymer was estimated using Flory-Huggins lattice theory.
Results. Nifedipine crystallized more readily than felodipine from the metastable amorphous form both alone and in the presence of PVP despite having a similar glass transition temperature and molecular mobility. Nifedipine was found to have a larger enthalpic driving force for crystallization and a lower activation energy for nucleation.
Conclusions. The properties of the metastable form alone did not explain the greater propensity for nifedipine crystallization. When considering the physical stability of amorphous systems, it is important to also consider the properties of the crystalline counterpart.

KEY WORDS: amorphous; crystallization; inhibition; nucleation; poly(vinylpyrrolidone).

INTRODUCTION

The importance of amorphous materials in pharmaceutical systems stems from their higher apparent solubility and faster dissolution rates which may lead to higher bioavailability (1–6). These enhanced properties come at the cost of decreased physical and chemical stability relative to the crystalline counterpart.

Polymers are commonly mixed at the molecular level with an amorphous drug in order to enhance physical stability (4,7–16). The influence of a polymer on the crystallization rate of amorphous drugs is typically described in terms of properties of the amorphous metastable form such as glass transition temperature (T_g), molecular mobility, and the interactions occurring between the drug and the polymer. For instance, several studies have shown improved physical stability with an increased glass transition temperature (7,9,10) although enhanced stability has also been shown in the absence of an increase in T_g for low polymer concentrations (17). Physical stability has also been attributed to the ability of the drug to form specific interactions with the polymer such as hydrogen bonding and ion-dipole interactions (10,11,18). However, the argument has also been made that if an amorphous drug is stable in the absence of a polymer, it will remain stable in the presence of a polymer regardless of whether specific interactions are present (8,9,13). Although many of these factors are related and the problem is complicated, it is clear that the increased physical stability of amorphous materials must be related to both the free energy of the amorphous material relative to the crystalline state (i.e., the thermodynamic driving force for crystallization) and factors which affect the kinetics of crystallization. Therefore, studies in this area should include not only an examination of the properties of the metastable amorphous form but also probe how the polymer influences the thermodynamics and kinetics of the crystal nucleation event. The rationale behind this statement is that amorphous molecular level solid dispersions will only find utility if physical stability is preserved through inhibition of the events leading to bulk crystallization with the initiating event being nucleation.

The objective of this study was to investigate thermodynamic, kinetic and structural factors contributing to the differences between the isothermal nucleation rates of two structurally related calcium channel blockers, nifedipine and felodipine, both alone and in the presence of poly(vinylpyrrolidone) (PVP). In the absence of PVP, the thermodynamic

[1] Department of Industrial and Physical Pharmacy, School of Pharmacy, Purdue University, West Lafayette, Indiana 47907, USA.
[2] Present address: Astellas Pharma Inc., 2-1-6 Kashima, Yodogawa-ku, Osaka 532-8514, Japan.
[3] To whom correspondence should be addressed. (e-mail: ltaylor@pharmacy.purdue.edu)

differences between the amorphous and crystalline forms are easily determined using thermal analysis. In the presence of PVP, the thermodynamic differences between the amorphous and crystalline forms are more difficult to elucidate. However, a discussion of the change in drug activity as a function of polymer concentration in the amorphous molecular level dispersion is presented in terms of Flory-Huggins lattice theory (19) and provides some insight into the implications of mixing on the nucleation event. Kinetic factors contributing to the differences between the isothermal crystallization rates of each drug both alone and in the presence of PVP are described in terms of the activation energy, as measured by an Arrhenius plot of the nucleation rate as a function of temperature, and the more common "metrics" used to describe the dynamics of amorphous molecular level solid dispersions; molecular mobility and the glass transition temperature. Finally, the molecular level structure of the systems was examined in terms of hydrogen bonding interactions using infrared (IR) spectroscopy.

MATERIALS

Felodipine was a generous gift from AstraZeneca, Södertälje, Sweden, and nifedipine was obtained from Hawkins, Inc, Minneapolis, MN, USA. Poly(vinylpyrrolidone) K29/32 (PVP) and acetone were purchased from Sigma-Aldrich Co., St. Louis, MO, USA. Dichloromethane and ethanol were obtained from Mallinckrodt Baker, Inc., Paris, KY, USA and Aaper Alcohol and Chemical Co., Shelbyville, KY, USA, respectively. The chemical structure of the felodipine, nifedipine, and PVP are given in Fig. 1.

MATERIALS AND METHODS

Preparation of Spin-Coated Films

Spin-coating was performed using KW-4A spin-coater (Chemat Technology Inc., Northridge, CA, USA) inside a glovebox at a relative humidity of less than 10%. Nifedipine or felodipine and PVP K29/32 were dissolved together in a suitable solvent; 50:50 wt.% dichloromethane:ethanol or acetone. A small drop of the solution was then placed on a clean, rotating substrate and the resulting film was heated to 90°C for several minutes to remove volatiles and then immediately placed in a desiccator at 0% relative humidity. Thin films were prepared on ZnS substrates for IR measurement and glass substrates for optical microscope studies. This procedure resulted in optically transparent films.

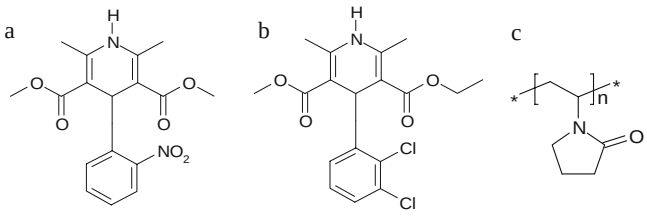

Fig. 1. Chemical structure of nifedipine (a), felodipine (b), and repeat unit of PVP (c).

Preparation of Bulk Amorphous Materials

Amorphous felodipine and nifedipine were prepared for thermal analysis by *in situ* melting and cooling of the crystalline material in the differential scanning calorimeter (DSC). Amorphous molecular level dispersion of the drugs and the polymer were prepared by solvent evaporation. Nifedipine or felodipine and PVP were dissolved in 100% ethanol and solvent removal was accomplished using a rotary evaporator apparatus (Brinkman Instruments, Westbury, NY, USA). The samples were placed under vacuum for at least 12 h prior to DSC measurement to ensure removal of any residual volatiles.

Evaluation of Nucleation Rate with Optical Microscopic Observation

Spin-coated samples were stored in desiccators over phosphorous pentoxide (0% RH) at 22°C. Samples were removed from the desiccators at each time point and the nucleation site number density was determined using an Olympus BHS polarized light microscope at 10×–50× magnification (Olympus Co., Tokyo, Japan). A total of 12 different sections of the film were analyzed for each of the triplicate samples at each time point. The site number density per unit volume was calculated from the site number density per unit area and the depth of field of the appropriate lens (20). The depth of field (D_{tot}) as a function of the wavelength of the light used (λ = 550 nm) and the numerical aperture (NA) of the lens is given in Eq. 1 (21).

$$D_{tot}=\frac{\lambda n}{NA^2}+\frac{n\cdot e}{M\cdot NA} \quad (1)$$

Where n is the refractive index of the medium (n_{air} = 1.000), e is the smallest distance that can be resolved by a detector (e = 14 μm) and M is lateral magnification. For example, based on these calculations, D_{tot} was 0.0144 mm for 10× objective.

In some cases preferential nucleation and growth appeared at the periphery of the films; these sites were not included in the analysis.

Evaluation of Activation Energy for Nucleation

Activation energies for nucleation, ΔE, were calculated by measuring the temperature dependence of the nucleation rate, I, for each amorphous compound according to the Arrhenius relationship (Eq. 2).

$$I=A\exp\left(-\frac{\Delta E}{RT}\right) \quad (2)$$

Where A is the pre-exponential factor, R is the universal gas constant, and T is the absolute temperature.

Infrared Spectroscopy

FT-IR spectra of the amorphous molecular level dispersions spin-coated onto ZnS substrates were collected on a Bio-Rad FTS-6000 (Bio-Rad, Cambridge, MA, USA). Reference spectra of the pure amorphous compound were

obtained by spin coating a thin film followed by melting and cooling. Spectra of reference crystalline materials were acquired after spin coating a film and allowing the drugs to completely crystallize. All sample preparation was performed in glove box under dry nitrogen gas. 128 scans were averaged at a resolution of 4 cm^{-1} for each sample over the wave number region 4,500–400 cm^{-1}. The optics and sample compartment were purged with dry, CO_2-free air to prevent absorption of moisture into the sample and other spectral interference from water vapor and CO_2.

Glass Transition Temperature and Heat Capacity Measurements

Glass transition temperature (T_g) and heat capacity measurements were made with a TA 2920 Modulated DSC equipped with a refrigerated cooling accessory (TA Instruments, New Castle, DE, USA). In both standard mode and modulated mode the instrument was calibrated for temperature using benzophenone (Sigma-Aldrich Inc., St. Louis MO, USA) and indium (Perkin-Elmer Corporation, Norwalk, CT, USA) and the enthalpic response was calibrated using indium. Nitrogen, 45 ml/min, served as the purge gas in standard mode while helium, 25 ml/min, was used in modulated mode. The heat capacity constant was calculated at an underlying heating rate of 2 K/min, an amplitude of 0.5 K, and a period of 1 min using a sapphire standard (Rheometric Scientific, Piscataway, NJ, USA). The same pan was used for both the sapphire standard and the sample to avoid differences associated with different pans. Heat capacity constants were calculated as a function of temperature by comparing measured values to those obtained using microthermal calorimetry as provided by TA instruments (TA Instruments, New Castle, DE, USA). Aluminum pans with a small pin-hole were used for all experiments and were matched for weight to within 0.01 mg.

Enthalpy, Entropy and Free Energy of Crystallization

The change in free energy upon crystallization, ΔG_C, was estimated using the Hoffman equation which was derived for temperatures above T_g by assuming that the enthalpy of the supercooled liquid and the crystal follow a linear relationship with temperature (Eq. 3) (22).

$$\Delta G_c = \Delta H_f \frac{(T_M - T)T}{{T_M}^2} \tag{3}$$

Here, ΔH_f is the enthalpy of fusion, T_M is the melting temperature. Since there is some curvature to the heat capacity as a function of temperature and a significant decrease in the heat capacity at the glass transition temperature, a more exact calculation can be made by measuring the heat capacity of the supercooled liquid and glassy materials as a function of temperature. The configurational heat capacity (C_p^{config}) is calculated as the difference in heat capacity between the supercooled liquid or the glass and the crystalline material, from which the configurational enthalpy (H_C), entropy (S_C), and free energy (G_C) were calculated as shown in Eqs. 4, 5, and 6 with $\Delta S_f = \Delta H_f / T_M$.

$$\Delta H_c = \Delta H_f + \int_{T_M}^{T} Cp^{config} dT \tag{4}$$

$$\Delta S_C = \Delta S_f + \int_{T_M}^{T} \frac{Cp^{config}}{T} dT \tag{5}$$

$$\Delta G_C(T) = H_c(T) - TS_c(T) \tag{6}$$

Molecular Mobility

The molecular mobility of amorphous nifedipine, felodipine, and amorphous molecular level dispersions with PVP were estimated using differential scanning calorimetry (23–25). Specifically, the enthalpy recovered as the glass approached the supercooled metastable liquid, $\Delta H_{t,T}$, was measured following aging for different periods of time at a temperature of 23.5°C. Data were fit to the Kohlrausch–Williams–Watts equation (Eq. 7) (26).

$$\frac{\Delta H_{t,T}}{\Delta H_{max,T}} = 1 - \exp\left(-\frac{t}{\tau}\right)^{\beta} \tag{7}$$

This equation describes relaxation processes as a function of time, t, in terms of a mean relaxation time constant, τ, a constant β, and the maximum amount of enthalpy recovered at infinite time, $\Delta H_{max,T}$. The latter term is related to the difference in the heat capacity of the supercooled liquid and the glass, ΔC_P^{Tg}, as shown in Eq. 8.

$$\Delta H_{max,T} = \Delta C_P^{T_g}(T_g - T) \tag{8}$$

The fraction of the total enthalpy recovered at a particular storage temperature was then calculated at each time point and fit to Eq. 7 from which the characteristic relaxation time constant and the exponential correction terms were estimated. This approach has been used widely for single component systems, and has also been applied to binary systems including polymer–polymer blends and polymer–drug blends (27–29).

RESULTS

Amorphous Nifedipine *vs.* Amorphous Felodipine in the Absence of PVP

Nucleation Rate Analysis for Pure Amorphous Felodipine and Nifedipine

Figure 2 shows the nucleation site number density per unit volume for nifedipine and felodipine as a function of time stored at 22°C and 0% RH. The number of nucleation sites increases linearly with time and the slope is equal to the

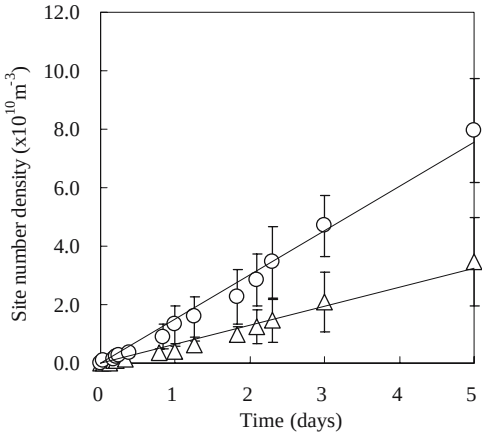

Fig. 2. Nucleation site number density as a function of time at 22°C and 0% RH for nifedipine (○) and felodipine (△) determined using optical microscopy. *Lines* determined by linear regression represent steady state nucleation rates. *Error bars* represent one standard deviation.

nucleation rate. From these data it can be seen that nifedipine has a more rapid nucleation rate from the amorphous form than felodipine at 22°C. Figure 3 shows the relationship between the natural logarithm of the nucleation rate and the inverse of temperature and it can be seen that the faster nucleation rate of nifedipine persists over the temperature range studied which covers regions above and below T_g. Although ΔE is not statistically different for the two compounds above T_g, ΔE for felodipine is significantly greater than that of nifedipine at temperatures below the T_g (Table I). It can also be noted from Fig. 3 that the trend in nucleation rate as a function of temperature displays a break at T_g for both compounds such that the nucleation rate dependence on temperature is much greater below T_g. This translates to higher activation energy for nucleation in the temperature region just below T_g relative to that just above T_g, presumably as a consequence of the higher molecular mobility above T_g.

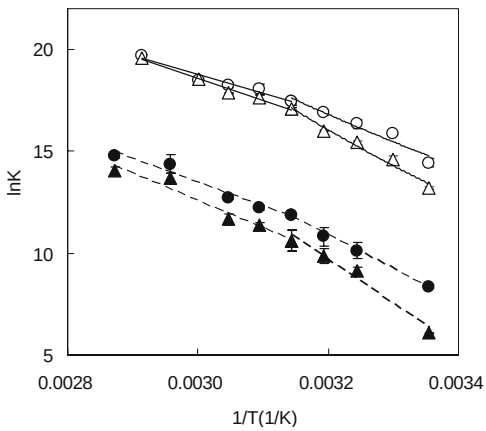

Fig. 3. Arrhenius plots of nucleation rate as a function of inverse temperature to determine activation energy for nucleation both above and below the glass transition temperature. *Symbols* represent nifedipine alone (○) or with 3 wt.% of PVP (●), and felodipine alone (△) or with 3 wt.% of PVP (▲). *Error bars* represent one standard deviation.

Non-Isothermal Crystallization

As further support for the enhanced crystallization tendency of nifedipine relative to felodipine, it was observed that a melt quenched sample of nifedipine crystallized to its metastable polymorph at 87 (+/−1)°C following heating through T_g at a heating rate of 2°C min^{-1} as compared to felodipine which showed no exothermic event and no melting endotherm following the same heating regimen (data not shown).

Glass Transition Temperature

As shown in Table II, the glass transition temperature of nifedipine is very similar to that of felodipine as measured by DSC with nifedipine having a slightly lower T_g than felodipine.

Molecular Mobility

The molecular mobility of felodipine and nifedipine as measured by DSC at 23.5°C in the absence of moisture was found to be very similar (Fig. 4). Specifically, the β and τ values were 0.36 (+/−0.01) and 6.3 (+/−0.3) h for nifedipine and 0.37 (+/−0.01) and 4.2 (+/−0.6) h for felodipine, respectively. It is immediately obvious that differences in crystallization tendency cannot be explained by differences in molecular mobility estimated using this commonly employed approach.

Enthalpy, Entropy, and Free Energy

The difference in free energy between the crystalline phase and the amorphous form provides the driving force for crystallization. Figure 5 shows the heat capacity of supercooled, glassy, and crystalline felodipine as a function of temperature. From these data, the configurational heat capacity was calculated as a function of temperature as shown in Fig. 6. Because amorphous nifedipine begins to recrystallize at 87 (+/−1)°C, the configurational heat capacity was extrapolated from this point to the melting temperature assuming a linear relationship as a function of temperature. The enthalpy and entropy differences were then calculated as a function of temperature using Eqs. 4, 5, and 6 and the resulting free energy difference is shown in Fig. 7. These data agree well with the predictions made by the Hoffman equation (Eq. 3) as shown in Table II and Fig. 7 (22).

Table I. Activation Energy for Nucleation of Pure Amorphous Nifedipine and Felodipine and their Amorphous Molecular Level Dispersions with 3 wt.% PVP

Sample	Activation Energy ΔE (kJ/mol)	
	Above T_g	Below T_g
Nifedipine	78 (8)	122 (11)
Felodipine	95 (12)	145 (3)
Nifedipine with 3% PVP	103 (5)	127 (15)
Felodipine with 3% PVP	111 (8)	201 (8)

Values in parentheses are standard deviations, $n = 3$.

Table II. A Comparison of Various Properties of Nifedipine and Felodipine

	Felodipine	Nifedipine
Nucleation rate (#/m^3/day)	0.17 (0.07)·10^{10}	0.39 (0.09)·10^{10}
T_m (°C)	141.6 (0.4)	172.1 (0.1)
T_g^{onset} (°C),	43.1 (0.5),	42.3 (0.3),
$T_g^{midpoint}$ (°C),	46.4 (0.3),	45.5 (0.3),
T_g^{offset} (°C)	48.9 (0.3)	47.7 (0.2)
ΔC_p^{Tg} (J/mol/°C)*	0.32 (0.01)	0.35 (0.01)
ΔH_{fus} (kJ/mol)	30.8 (1.1)	39.9 (1.1)
ΔS_{fus} (J/mol/°C)	74.4 (2.6)	89.6 (2.4)
$\Delta H_{25°C}$ (kJ/mol)	16.1 (1.9)	22.1 (1.1)
$\Delta S_{25°C} \cdot 298°C$ (kJ/mol)	10.0 (1.3)	12.5 (0.3)
$\Delta G_{25°C}$ (kJ/mol)	6.2 (2.1)	9.6 (0.6)
$\Delta G_{Hoffman25°C}$ (kJ/mol)	6.2 (0.2)	8.8 (0.2)
β	0.37 (0.01)	0.36 (0.01)
τ (h^{-1})	4.2 (0.6)	6.3 (0.3)

*Heat capacity change at the glass transition temperature ($C_p^{SCL} - C_p^{Glass}$). Values in parentheses are standard deviations, $n = 3$.

The free energy difference between the pure amorphous and crystalline forms of nifedipine is greater than that for the equivalent felodipine forms, hence nifedipine has a larger thermodynamic driving force for crystallization. As is apparent from Table II, this difference between the two compounds is due to the enthalpic component of the free energy change associated with the transition since nifedipine has a larger loss of entropy on crystallization (unfavorable to crystallization) than felodipine.

Hydrogen Bonding Patterns

The average strength of the hydrogen bonds in the pure amorphous form are very similar for nifedipine and felodipine as indicated by the peak position of the NH stretching frequency measured using IR spectroscopy (Fig. 8). However, there appears to be a slightly broader distribution of strengths of hydrogen bonds in nifedipine as indicated by the greater breadth of the NH peak for amorphous nifedipine relative to that of amorphous felodipine. For nifedipine, the hydrogen bonding in the crystalline state is stronger, on average, than in the amorphous form as indicated by a lower NH stretching frequency in the crystalline state (30,31,32). Conversely, the average strength of hydrogen bonding in the amorphous form of felodipine is stronger than in the crystalline form as indicated by a lower NH stretching frequency in the amorphous form. This observation is consistent with previous work by Tang *et al*. (33) and may provide some insight into the molecular level differences between the two compounds.

Amorphous Molecular Level Dispersions of Nifedipine and Felodipine in the Presence of PVP

Nucleation Rate Analysis for Amorphous Molecular Level Dispersions with PVP

The nucleation rates of the solid dispersions as a function of PVP concentration were obtained in the same manner as for the pure amorphous compounds. As shown in Fig. 9, PVP was found to dramatically reduce nucleation rates in the amorphous solid dispersions with an initial large reduction in nucleation rate at 7% PVP followed by a less dramatic reduction with increasing polymer concentration above 7% PVP. It should be noted that moisture has been rigorously excluded from these systems as far as possible. Furthermore, there is little difference in the stabilizing ability of PVP against nucleation in nifedipine and felodipine as a function of concentration (i.e., the extent of the reduction in nucleation rate upon addition of polymer is similar in each case). However, all solid dispersions with nifedipine maintain a higher nucleation rate than the equivalent felodipine solid dispersions, as was observed for the pure compounds. Finally, the average values all trend towards increased ΔE for both compounds with the addition of 3% PVP although it should be noted that while the experiments show a statistically significant increase in ΔE with the addition of 3% PVP for felodipine below T_g and nifedipine above T_g, they do not show a statistically significant increase in ΔE with the addition of 3% PVP for felodipine above T_g and nifedipine below T_g.

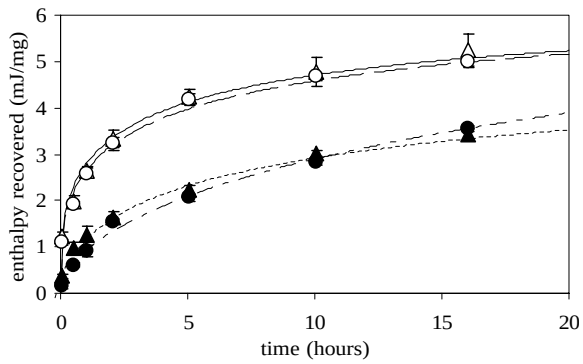

Fig. 4. Enthalpy recovered (mJ/mg) as a function of storage time at 23.5°C for nifedipine (○), felodipine (△), and amorphous molecular level solid dispersions of nifedipine with 10 wt.%PVP (●) and felodipine with 10 wt.%PVP (▲). *Error bars* represent one standard deviation.

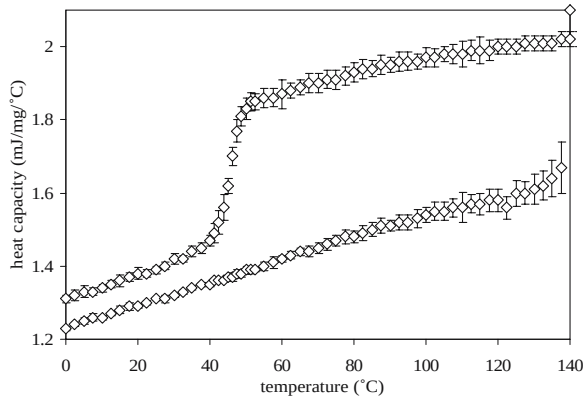

Fig. 5. Heat capacity of crystalline (*bottom*) and amorphous felodipine (*top*) as a function of temperature. The difference in heat capacity at each temperature gives the configurational heat capacity. *Error bars* represent one standard deviation.

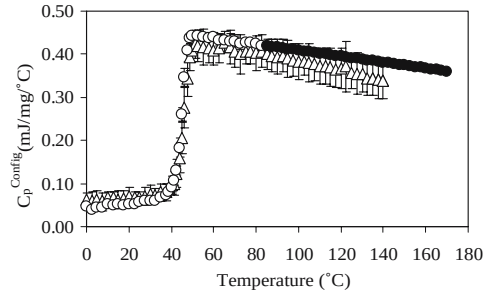

Fig. 6. Configurational heat capacity of nifedipine (○) and felodipine (△) as a function of temperature. The heat capacity of supercooled nifedipine was extrapolated using a linear relationship from the non-isothermal crystallization temperature, 87 (+/−1)°C, to the melting temperature, 172.1 (+/−0.1)°C. *Error bars* represent one standard deviation.

Glass Transition Temperature

The glass transition temperatures of amorphous molecular level solid dispersions of nifedipine and felodipine in the presence of PVP are shown in Fig. 10. The lines show the fit of the Gordon–Taylor (34) and Couchman Karaz (35,36) equations and it can be seen that both felodipine-PVP and nifedipine-PVP systems are relatively ideal in the context of these predictions. The antiplasticizing effect of PVP, with a glass transition temperature of 168 (+/−2)°C is clearly shown for all concentrations except at the 10 wt.% level of PVP with felodipine where the T_g is actually slightly lower than for the pure material. The lack of anti-plasticization of a low molecular weight material by small concentrations of a polymer has been observed previously (17,37). The presence of a single T_g for all mixture compositions indicates that the drug–polymer systems were miscible across the entire concentration range. For all concentrations, the T_gs of nifedipine-PVP solid dispersions are virtually identical to the T_gs of the equivalent felodipine-PVP systems.

Molecular Mobility

As shown in Fig. 4, a decrease in the enthalpy recovery as a function of time was observed for both nifedipine and felodipine in the presence of PVP at 23.5°C under dry conditions. The β and τ values were estimated as described above and gave values of 0.57 (+/−0.03) and 42.1 (+/−0.6) h for nifedipine with 10% PVP and 0.45 (+/−0.04) and 16.7 (+/−0.5) h for felodipine with 10% PVP, respectively.

Interestingly, the absolute enthalpy recovered was virtually identical for amorphous molecular level dispersions of nifedipine and felodipine containing 10 wt.% PVP. It can also be noted that for the felodipine/PVP system reduced mobility occurs despite a slight decrease in the T_g (T_g=43.1°C (+/−0.5) for pure felodipine and 40.5°C (+/−0.5) for felodipine with 10% PVP). More specifically, pure felodipine recovers about 5.4 (+/−0.3) mJ/mg enthalpy after 16 h and its expected maximum enthalpy recovery is 6.3 (+/−0.3) mJ/mg giving a total of 84% total recovery. Alternatively, felodipine with 10% PVP recovers about 3.4 (+/−0.1) mJ/mg enthalpy after 16 h and its expected maximum enthalpy recovery is 5.3 (+/−0.3) mJ/mg giving a total of 65% total recovery highlighting the fact that T_g alone does not completely describe the reduction in molecular mobility. These observations are in good agreement with other studies on binary mixtures of small molecules and polymers (28).

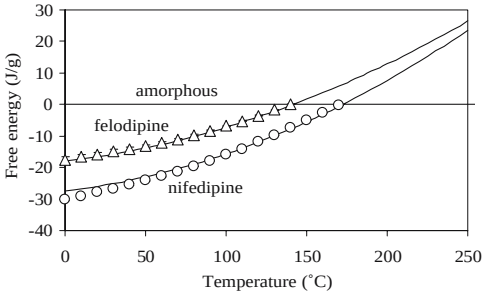

Fig. 7. Thermodynamic driving force for crystallization as represented by the difference in free energy between amorphous and crystalline nifedipine (○) and felodipine (△) as measured by MDSC and compared to the values predicted using the Hoffman equation (*solid lines*). *Error bars* represent one standard deviation and are smaller than the size of the symbol in some cases.

Hydrogen Bonding Patterns

FT-IR spectra of nifedipine and felodipine both in the amorphous form and in the presence of PVP were measured and are shown in Fig. 11. For the felodipine systems, three different states of NH stretch can be identified. The shoulder at 3,420 cm^{-1} is associated with free NH moieties while the peak at 3,345 cm^{-1} is associated with the drug hydrogen bonding with other drug molecules (33). With increasing PVP concentration, a shoulder arises and then a peak develops at 3,288 cm^{-1}. This peak can be assigned to drug–polymer

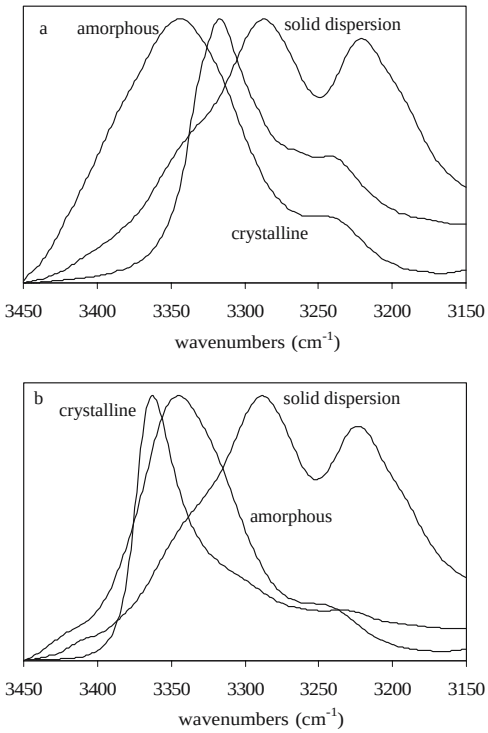

Fig. 8. FT-IR spectra of amorphous, crystalline, and amorphous molecular level dispersions at a 4:1 PVP hydrogen bond acceptor to hydrogen bond donor ratio for (a) nifedipine and (b) felodipine.

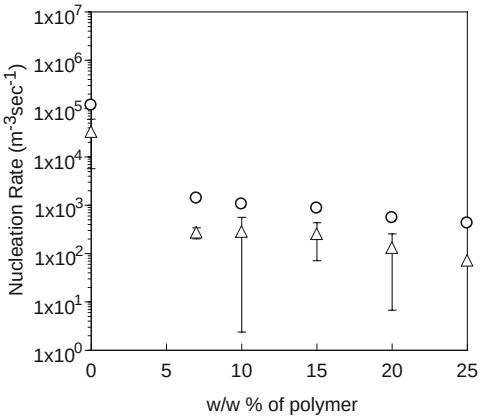

Fig. 9. Nucleation rate as a function of PVP concentration as determined from optical microscopy for amorphous molecular level solid dispersions of nifedipine with PVP (○) and felodipine with PVP (△). Samples were stored at 0%RH and *error bars* represent one standard deviation.

hydrogen bonding interactions, specifically the NH function hydrogen bonds with the carbonyl moiety in PVP. For nifedipine, the same phenomenon occurs with increasing PVP concentration. The development of this low wave number NH peak in the solid dispersions indicates that the drug–polymer hydrogen bonding interactions are stronger than those in the pure amorphous drugs. However, the interactions of each compound with PVP are very similar both in strength (as evidenced by the position of the peaks) and extent (as evidenced by the breadth of the peaks). The similarity in the interactions of the two compounds with PVP is shown by the peak height ratio of the peak arising from drug–drug interactions to that of the peak for the drug–polymer interactions as shown in Fig. 12. Note that in this plot, the peak height ratio is shown as a function of the molar ratio of polymer monomer unit to the drug. Thus, for a given number of hydrogen bond donors and acceptors, the interaction between drug and polymer is very similar. However, since nifedipine has a lower MW than felodipine, for a given weight percent of polymer, nifedipine would hydrogen bond to a greater extent than felodipine.

DISCUSSION

Factors Affecting the Relative Physical Stability of Amorphous Nifedipine and Felodipine

The rate of crystallization of nifedipine is clearly faster than that of felodipine despite having a virtually identical T_g and average relaxation time. Classical nucleation theory describes factors influencing nucleation kinetics from supercooled liquids (38). Specifically, the rate of nucleation has been described in terms of the free energy change for the formation of a nucleus of critical size, ΔG^* (representing the balance between the energy penalty associated with creating a new surface, ΔG_S, and the favorable reduction in free energy associated with forming a crystalline phase, ΔG_v), and the activation energy for transport of a molecule from the amorphous phase to the nucleus, ΔG_a (Eq. 9).

$$I = A \exp \frac{-(\Delta G^* + \Delta G_a)}{kT} \tag{9}$$

Where A is a constant, k is the Boltzmann constant, and T is the absolute temperature. It should be noted that the systems studied here are not completely described by the classical homogeneous nucleation equation since it does not account for (i) the stresses that develop in solid materials during the volume changes associated with nucleation (39,40) and (ii) the reduction in the thermodynamic barrier when nucleation is heterogeneous (40,41). Nevertheless, it serves as a tool to describe the balance between the thermodynamic driving force for nucleation, which increases with decreasing temperature, and kinetic factors, which become less favorable for nucleation as the temperature is reduced due to restricted molecular mobility. The two compounds differ in terms of the enthalpy, entropy, and free energy of crystallization as shown in Table II and Fig. 7. Nifedipine has the larger enthalpy of crystallization, which, being favorable to crystallization, would suggest that it would crystallize more readily. However, nifedipine also has greater entropy change on crystallization which is unfavorable to crystallization. The importance of the configurational entropy of crystallization has been discussed by Zhou *et al.* who found that materials with larger entropies of crystallization formed glasses which did not crystallize as readily under non-isothermal conditions (42). In the absence of a correlation between either the enthalpy of crystallization or the total thermodynamic driving

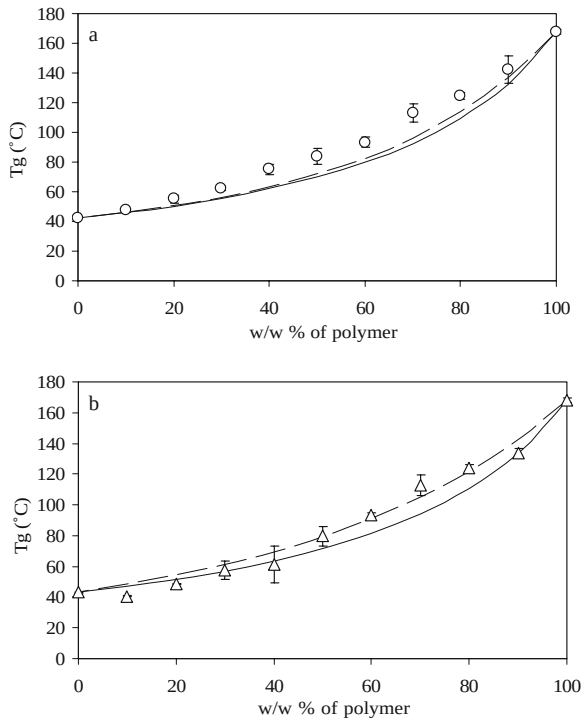

Fig. 10. Glass transition temperature of amorphous molecular level dispersions of (a) nifedipine in PVP (○) and (b) felodipine in PVP (△) as a function of weight fraction PVP and compared to the Couchman–Karasz equation (--) and Gordan–Taylor equation (—). *Error bars* represent one standard deviation.

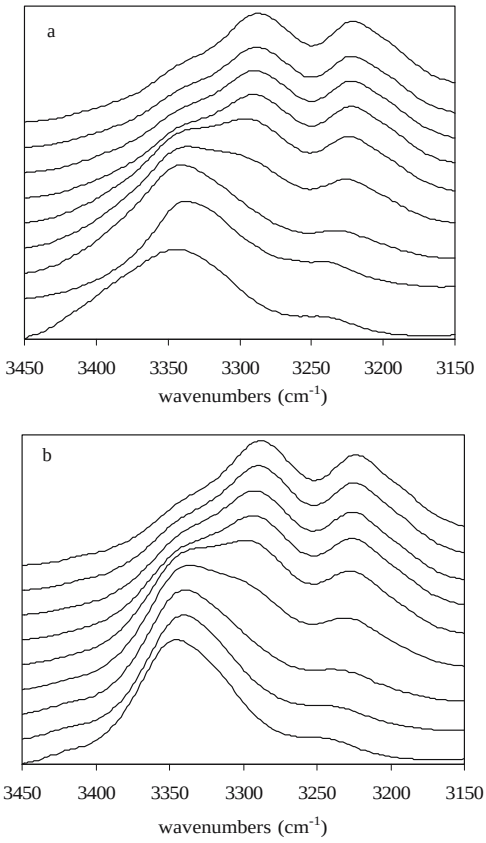

Fig. 11. FT-IR spectra of amorphous molecular level dispersions of nifedipine (a) and felodipine (b) with PVP at a PVP hydrogen bond acceptor to drug hydrogen bond donor ratio of (*from bottom to top*) 0, 0.25, 0.5, 1.0, 1.5, 2.0, 2.5, 3.0, and 4.0.

force, it was concluded that compounds with the highest entropic barriers were most resistant to crystallization. The importance of the entropy of crystallization may be interpreted as the probability that the molecule is in the correct conformation and/or orientation to act as a "building block" for nucleation. If crystallization tendency was dominated by entropy considerations as suggested previously (42), the thermodynamic analysis would suggest that felodipine should crystallize more easily. Results from this study do not follow this trend, and for this particular pair of compounds point to the importance of the enthalpy of crystallization which makes the dominating contribution to the free energy of crystallization.

The interfacial energy term, ΔG_S, is difficult to measure experimentally with any degree of certainty, particularly for glassy systems. Turnbull developed an empirical relationship for metallic materials which suggests that the crystal-melt interfacial energy is proportional to the enthalpy of fusion (43). Thus metals with a higher heat of fusion have a larger value of the crystal-melt interfacial tension and are more resistant to nucleation. Even if this relationship held true for organic molecular systems in the glassy state, it would not account for the difference in the nucleation rate between nifedipine and felodipine because nifedipine has the higher enthalpy of fusion which would result in a larger interfacial energy.

As stated earlier, thermodynamic factors do not provide a complete description of the nucleation tendency from highly viscous systems and kinetic and structural factors must also be considered. In glasses, the molecular mobility of molecules is restricted by the high viscosity. The observation that both the T_g and average relaxation times at 23.5°C are virtually identical for both compounds suggests either that other factors dictate the nucleation event or that this measure of molecular mobility does not provide a good description of the type of motion involved in the nucleation process. However, the observation that the activation energy for nucleation below T_g is higher for felodipine than nifedipine provides evidence that kinetic factors are also important in influencing the relative crystallization tendency of the compounds. There are also interesting differences in hydrogen bonding patterns. Tang *et al.* investigated the amorphous and crystalline hydrogen bonding patterns in a series of dihydropyridine calcium channel blockers including those used in this study (33). The FT-Raman and FT-infrared spectra showed that the hydrogen bonding strength varied between the crystalline forms of the compounds but was remarkably uniform for all the amorphous forms. While some of the materials, including nifedipine, showed stronger hydrogen bonding in the crystalline state than the amorphous form, others, including felodipine, exhibited stronger average hydrogen bonding in the amorphous form (consistent with the results presented here). These differences in hydrogen bonding strength between the crystalline and amorphous forms may influence the crystallization tendency. Specifically, as nifedipine crystallizes, the hydrogen bonding strength increases which would be expected to be favorable since the enthalpic interactions are increasing. In contrast, felodipine crystallizes at the expense of an average reduction in the strength of hydrogen bonding interactions. Thus it would be reasonable to speculate that the higher activation energy observed for felodipine relative to nifedipine might arise from the necessity of weakening hydrogen bonding prior to crystallization for a given population of amorphous molecules. The lower entropy of crystallization for felodipine may also be related to the hydrogen bonding differences in the amorphous and crystalline forms as has been suggested previously (44). Thus the increased nucleation rate of nifedipine relative to felodipine may arise either because there is a greater thermodynamic driving force or because there is a reduced energy barrier to nucleation or may be due

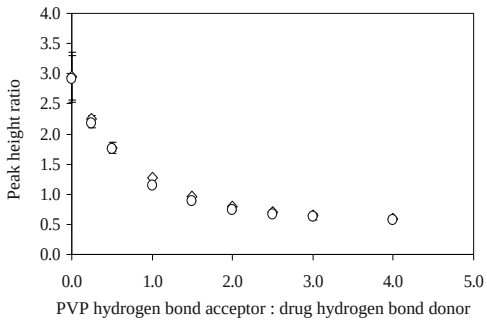

Fig. 12. Peak height ratio of NH stretching frequencies corresponding to drug–drug hydrogen bonding (3,345 cm^{-1}), and the drug-PVP hydrogen bonding (3,288 cm^{-1}), as a function of PVP hydrogen bond acceptor to drug hydrogen bond donor ratio. *Symbols* represent values for nifedipine with PVP (○) and felodipine with PVP (△). *Error bars* represent one standard deviation.

to a combination of both factors. Further investigations are necessary in order to establish if kinetic or thermodynamic factors dominate the observed difference in nucleation kinetics in the glassy region for these two compounds.

Factors Affecting the Relative Stability of Amorphous Nifedipine and Felodipine in the Presence of PVP

The stabilizing ability of a polymer has been described in the literature in terms of its ability to decrease free volume (37), decrease molecular mobility (24,45), increase the glass transition temperature (46), disrupt drug–drug interactions (11), and form drug–polymer interactions (10–12). In addition, some authors have described the stability of amorphous molecular level dispersions in terms of the crystallization tendency of the pure amorphous drug (8,9,13). We have made an attempt to assess the influence of these various factors on the crystallization behavior of felodipine and nifedipine from solid dispersions with PVP, however, in reality it should be noted that many of these factors are interrelated. As presented above, it was found that nifedipine-PVP solid dispersions had faster nucleation rates than the equivalent felodipine-PVP solid dispersions for all polymer concentrations investigated. Furthermore, many of the factors listed above were either observed to be similar for solid dispersions of the two compounds or not to correlate in the expected manner with the nucleation rates: T_g as a function of polymer weight percent was roughly equal in each system, enthalpy recovery experiments gave similar results, and the extent of drug–polymer interactions were slightly higher for nifedipine-PVP systems (at a given weight fraction). Thus, as for the pure substances, some common "metrics" of crystallization tendency were not predictive of the observed differences between nifedipine and felodipine solid dispersions. It is of interest to consider these two systems in more depth in terms the factors in Eq. 9 that might be changed by the presence of the polymer.

A single glass transition temperature and the presence of drug–polymer interactions over all compositions demonstrate miscibility. Therefore, the molecular level environment of the drug is altered leading to potential changes in the thermodynamic driving force for crystallization (ΔG_v term), the energy penalty for creating a new interface (ΔG_s) and the activation energy (ΔE).

Consider first the thermodynamic driving force for crystallization. Complete miscibility requires that the activity of the drug in the polymer matrix is reduced relative to the activity of the pure amorphous drug. Therefore, the thermodynamic driving force for crystallization must be reduced (47). Using solution theory based models for binary mixtures, the magnitude of the activity reduction for felodipine and nifedipine in PVP solid dispersions can be compared.

Flory–Huggins (FH) lattice theory was developed to describe the activity of a solvent in a polymer solution (19). If the amorphous drug is assumed to be equivalent to the solvent, then FH theory can be used to approximate the change in the activity of the drug as a function of polymer concentration. Although there are certain well know limitations of FH theory (19,48) and the systems under consideration are non-equilibrium glasses, this analysis can provide a basis for comparison of nifedipine and felodipine activity changes in the presence of PVP. The reduction in activity of nifedipine and felodipine in the presence of PVP can be calculated as shown in Eq. 10.

$$\ln a_{drug} = \ln \Phi_{drug} + \left(1-\frac{1}{m}\right)\Phi_{PVP} + \chi\Phi_{PVP}^2 \qquad (10)$$

Where a_{drug} is the activity of the drug in the polymer matrix, Φ_{drug} is the volume fraction of the drug, m is the ratio of the molecular volume of PVP to that of the drug, Φ_{PVP} is the volume fraction of PVP and χ is the interaction parameter between the drug and PVP. Interaction parameters of −3.8 and −4.2 were used for nifedipine-PVP and felodipine-PVP, respectively. These values have been previously estimated for the systems under investigation (49) using melting point depression methods (50,51).

Figure 13 shows that the predicted reduction in activity of the drug is very similar for both nifedipine and felodipine. In addition, the magnitude of activity reduction predicted by the method described above is small for the range of polymer concentrations used in this study. Therefore, based strictly on a potential change in ΔG_v, it would be expected that, at any particular polymer concentration, the rate of nucleation of nifedipine would still exceed that of felodipine since the energy gain of forming crystalline nifedipine would be greater than for felodipine, as for the pure drugs.

For the solid dispersions, the average activation energy trended towards higher values relative to that of the pure drug (although it was found that the difference is not statistically significant for nifedipine below T_g and felodipine above T_g) (Table I). Furthermore, as was observed for the pure drugs, the felodipine-PVP solid dispersion was found to have a higher ΔE value than the corresponding nifedipine system below T_g. Hence it appears that the energetic barrier for nucleation is higher in felodpine than in nifedipine both in the presence and absence of the polymer.

It is apparent from the results presented herein that the relative physical stability of the two model compounds is not explained by differences associated with the various properties of the metastable amorphous form that were measured in this study. The relative physical stability did however correlate with the larger enthalpic driving force for crystallization of nifedipine and the relatively lower activation energy for crystallization in nifedipine systems. Therefore when considering the physical stability of amorphous systems, it is important to consider not only the properties of the supercooled liquid/glass but also how these relate to those of the crystalline counterpart. This concept has been invoked

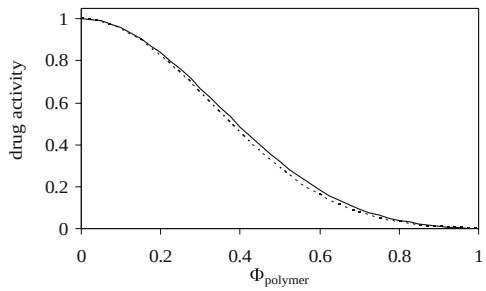

Fig. 13. Thermodynamic activity of amorphous nifedipine (—) and felodipine (- -) as a function of volume fraction PVP as predicted using Flory–Huggins lattice theory.

when discussing the glass forming tendency of molecular liquids supercooled from the melt (52). Results presented in this study would also support the conjecture that for a given class of amorphous materials, the greater the tendency of an amorphous phase to crystallize, then the larger the concentration of polymeric stabilizer necessary to produce a certain extent of physical stabilization.

CONCLUSIONS

Nifedipine crystallizes more readily than felodipine both from the pure amorphous form and out of amorphous molecular level dispersions with PVP (at equivalent polymer concentrations). This greater ease of nifedipine crystallization from the amorphous form could not be anticipated by considering commonly used metrics such as T_g and molecular mobility as measured by DSC since these were virtually identical for the two drugs. It was found that the thermodynamic driving force for crystallization of nifedipine is greater than that of felodipine despite the former compound having a larger entropic barrier to crystallization. Furthermore, the activation energy for nucleation of nifedipine was lower than that of felodipine below the glass transition temperature. Solid dispersions of both drugs also showed very similar amorphous properties which were therefore not indicative of relative physical stability. It is concluded that the relative crystallization tendency of drugs from solid dispersions may be dependent on the relative crystallization tendencies of the pure substances.

ACKNOWLEDGEMENTS

Professor George Zografi is thanked for many enlightening discussions about this research. The authors are grateful to Dr Sheri L. Shamblin for helpful comments. The PhRMA Foundation is acknowledged for a pre-doctoral fellowship to PJM. LST thanks AFPE/AACP for a New Investigator Award. HK acknowledges Astellas Pharma Inc. for granting him a leave of absence to undertake this work. AstraZeneca is thanked for financial support.

REFERENCES

1. W. L. Chiou and S. Riegelman. Pharmaceutical applications of solid dispersion systems. *J. Pharm. Sci.* **60**:1281–1302 (1971).
2. J. L. Ford. The current status of solid dispersions. *Pharm. Acta Helv.* **61**:69–88 (1986).
3. L. Yu. Amorphous pharmaceutical solids: preparation, characterization and stabilization. *Adv. Drug Deliv. Rev.* **48**:27–42 (2001).
4. D. Law, E. A. Schmitt, K. C. Marsh, E. A. Everitt, W. L. Wang, J. J. Fort, S. L. Krill, and Y. H. Qiu. Ritonavir-PEG 8000 amorphous solid dispersions: *in vitro* and *in vivo* evaluations. *J. Pharm. Sci.* **93**:563–570 (2004).
5. A. T. M. Serajuddin. Solid dispersion of poorly water-soluble drugs: early promises, subsequent problems, and recent breakthroughs. *J. Pharm. Sci.* **88**:1058–1066 (1999).
6. S. Sethia and E. Squillante. Solid dispersions: revival with greater possibilities and applications in oral drug delivery. *Crit. Rev. Ther. Drug Carr. Syst.* **20**:215–247 (2003).
7. T. Miyazaki, S. Yoshioka, Y. Aso, and S. Kojima. Ability of polyvinylpyrrolidone and polyacrylic acid to inhibit the crystallization of amorphous acetaminophen. *J. Pharm. Sci.* **93**:2710–2717 (2004).
8. I. Weuts, D. Kempen, A. Decorte, G. Verreck, J. Peeters, M. Brewster, and G. Van den Mooter. Phase behaviour analysis of solid dispersions of loperamide and two structurally related compounds with the polymers PVP-K30 and PVP-VA64. *Eur J Pharm Sci* **22**:375–385 (2004).
9. G. Van den Mooter, M. Wuyts, N. Blaton, R. Busson, P. Grobet, P. Augustijns, and R. Kinget. Physical stabilisation of amorphous ketoconazole in solid dispersions with polyvinylpyrrolidone K25. *Eur. J. Pharm. Sci.* **12**:261–269 (2001).
10. K. Khougaz and S. D. Clas. Crystallization inhibition in solid dispersions of MK-0591 and poly(vinylpyrrolidone) polymers. *J. Pharm. Sci.* **89**:1325–1334 (2000).
11. L. S. Taylor and G. Zografi. Spectroscopic characterization of interactions between PVP and indomethacin in amorphous molecular dispersions. *Pharm. Res.* **14**:1691–1698 (1997).
12. V. Tantishaiyakul, N. Kaewnopparat, and S. Ingkatawornwong. Properties of solid dispersions of piroxicam in polyvinylpyrrolidone K-30. *Int. J. Pharm.* **143**:59–66 (1996).
13. D. Law, S. L. Krill, E. A. Schmitt, J. J. Fort, Y. H. Qiu, W. L. Wang, and W. R. Porter. Physicochemical considerations in the preparation of amorphous ritonavir-poly(ethylene glycol) 8000 solid dispersions. *J. Pharm. Sci.* **90**:1015–1025 (2001).
14. H. Suzuki and H. Sunada. Influence of water-soluble polymers on the dissolution of nifedipine solid dispersions with combined carriers. *Chem. Pharm. Bull.* **46**:482–487 (1998).
15. S. Sethia and E. Squillante. Solid dispersion of carbamazepine in PVPK30 by conventional solvent evaporation and supercritical methods. *Int. J. Pharm.* **272**:1–10 (2004).
16. E. Broman, C. Khoo, and L. S. Taylor. A comparison of alternative polymer excipients and processing methods for making solid dispersions of a poorly water soluble drug. *Int. J. Pharm.* **222**:139–151 (2001).
17. K. J. Crowley and G. Zografi. The effect of low concentrations of molecularly dispersed poly(vinylpyrrolidone) on indomethacin crystallization from the amorphous state. *Pharm. Res.* **20**:1417–1422 (2003).
18. M. Fujii, J. Hasegawa, H. Kitajima, and M. Matsumoto. The solid dispersion of benzodiazepins with phosphatidylcholine—the effect of substituents of benzodiazepins on the formation of solid dispersions. *Chem. Pharm. Bull.* **39**:3013–3017 (1991).
19. P. J. Flory. *Principles of Polymer Chemistry*, Cornell University Press, Ithaca, 1953.
20. V. Andronis and G. Zografi. Crystal nucleation and growth of indomethacin polymorphs from the amorphous state. *J. Non-Cryst. Solids* **271**:236–248 (2000).
21. S. O. Inoue. Microscopes. *Handbook of Optics, Vol. II*, McGraw-Hill, New York, 1995.
22. J. D. Hoffman. Thermodynamic driving force in nucleation and growth processes. *J. Chem. Phys.* **29**:1192–1193 (1958).
23. I. M. Hodge. Enthalpy relaxation and recovery in amorphous materials. *J. Non-Cryst. Solids* **169**:211–266 (1994).
24. B. C. Hancock and S. L. Shamblin. Molecular mobility of amorphous pharmaceuticals determined using differential scanning calorimetry. *Thermochim. Acta* **380**:95–107 (2001).
25. B. C. Hancock, S. L. Shamblin, and G. Zografi. Molecular mobility of amorphous pharmaceutical solids below their glass-transition temperatures. *Pharm. Res.* **12**:799–806 (1995).
26. G. Williams and D. C. Watts. Non-symmetrical dielectric relaxation behaviour arising from a simple empirical decay function. *Trans. Faraday Soc.* **66**:80 (1970).
27. J. M. G. Cowie and R. Ferguson. Physical aging studies in polymer blends. 2. Enthalpy relaxation as a function of aging temperature in a polyvinyl methyl ether polystyrene blend. *Macromolecules* **22**:2312–2317 (1989).
28. S. L. Shamblin and G. Zografi. Enthalpy relaxation in binary amorphous mixtures containing sucrose. *Pharm. Res.* **15**:1828–1834 (1998).
29. T. Matsumoto and G. Zografi. Physical properties of solid molecular dispersions of indomethacin with poly(vinylpyrrolidone) and poly(vinylpyrrolidone-co-vinylacetate) in relation to indomethacin crystallization. *Pharm. Res.* **16**:1722–1728 (1999).

30. K. Nakamoto, M. Margoshes, and R. E. Rundle. Stretching frequencies as a function of distances in hydrogen bonds. *J. Am. Chem. Soc.* **77**:6480–6486 (1955).
31. G. A. Jeffrey. *An Introduction to Hydrogen Bonding*, Oxford University Press, New York, 1997.
32. Y. Aso and S. Yoshioka. Molecular mobility of nifedipine-PVP and phenobarbital-PVP solid dispersions as measured by 13C-NMR spin-lattice relaxation time. *J. Pharm. Sci.* **95**:318–325 (2006).
33. X. L. C. Tang, M. J. Pikal, and L. S. Taylor. A spectroscopic investigation of hydrogen bond patterns in crystalline and amorphous phases in dihydropyridine calcium channel blockers. *Pharm. Res.* **19**:477–483 (2002).
34. M. Gordon and J. S. Taylor. Ideal copolymers and the 2nd-order transitions of synthetic rubbers. 1. Non-crystalline copolymers. *J. Appl. Cheri.* **2**:493–500 (1952).
35. P. R. Couchman and F. E. Karasz. Classical thermodynamic discussion of effect of composition on glass-transition temperatures. *Macromolecules* **11**:117–119 (1978).
36. P. R. Couchman. Compositional variation of glass-transition temperatures. 2. Application of thermodynamic theory to compatible polymer blends. *Macromolecules* **11**:1156–1161 (1978).
37. S. L. Shamblin, L. S. Taylor, and G. Zografi. Mixing behavior of colyophilized binary systems. *J. Pharm. Sci.* **87**:694–701 (1998).
38. D. Turnbull and J. C. Fisher. Rate of nucleation in condensed systems. *J. Chem. Phys.* **17**:71–73 (1949).
39. J. C. Fisher, J. H. Hollomon, and D. Turnbull. Nucleation. *J. Appl. Physi.* **19**:775–784 (1948).
40. D. Kashchiev. *Nucleation; Basic Theory with Applications*, Butterworth Heinemann, Woburn, MA, 2000.
41. J. W. Mullin. *Crystallization*, Reed Educational and Professional Publishing, Oxford, 2001.
42. D. L. Zhou, G. G. Z. Zhang, D. Law, D. J. W. Grant, and E. A. Schmitt. Physical stability of amorphous pharmaceuticals: importance of configurational thermodynamic quantities and molecular mobility. *J. Pharm. Sci.* **91**:1863–1872 (2002).
43. D. Turnbull. Formation of crystal nuclei in liquid metals. *J. Appl. Physi.* **21**:1022–1028 (1950).
44. X. L. C. Tang, M. J. Pikal, and L. S. Taylor. The effect of temperature on hydrogen bonding in crystalline and amorphous phases in dihydropyrine calcium channel blockers. *Pharm. Res.* **19**:484–490 (2002).
45. K. J. Crowley and G. Zografi. The use of thermal methods for predicting glass-former fragility. *Thermochim. Acta* **380**:79–93 (2001).
46. D. Q. M. Craig, P. G. Royall, V. L. Kett, and M. L. Hopton. The relevance of the amorphous state to pharmaceutical dosage forms: glassy drugs and freeze dried systems. *Int. J. Pharm.* **179**:179–207 (1999).
47. C. V. Thompson and F. Spaepen. Homogeneous crystal nucleation in binary metallic melts. *Acta Metall.* **31**:2021–2027 (1983).
48. M. M. Coleman, J. F. Graf, Painter, and C. Paul. *Specific interactions and the miscibility of polymer blends*, Technomic Publishing AG, Lancaster, Pennsylvania, 1991.
49. P. J. Marsac, S. L. Shamblin, and L. S. Taylor. Theoretical and practical approaches for prediction of drug–polymer miscibility and solubility. Pharmaceutical Research in press: (2006).
50. T. Nishi and T. T. Wang. Melting-point depression and kinetic effects of cooling on crystallization in poly(Vinylidene Fluoride) poly(Methyl Methacrylate) mixtures. *Macromolecules* **8**:909–915 (1975).
51. E. Meaurio, E. Zuza, and J. R. Sarasua. Miscibility and specific interactions in blends of poly(L-lactide) with poly(vinylphenol). *Macromolecules* **38**:1207–1215 (2005).
52. D. Turnbull and M. H. Cohen. Free-volume model of amorphous phase—glass transition. *J. Chem. Phys.* **34**:120–125 (1961).